A Three Dimensional FDTD Algorithm for Wave Propagation in Cold Plasma Media using Forth-Order Schemes

M. Pourbagher[1] and S. Sohafi[2]

[1] Department of Electrical Engineering, Urmia University
armanpurbaqer@yahoo.com

[2] Department of Electrical Engineering, Semnan University

***Abstract*—** A fourth-order accurate in space and second-order accurate in time, finite-difference time-domain (FDTD) scheme for wave propagation in cold plasma media is presented. The formulation of Maxwell's equations is fully described and an elaborate study of the stability and dispersion properties of the resulting algorithm is conducted. The efficiency of the proposed FDTD (2, 4) technique in cold plasma media compared to its conventional FDTD (2, 2) counterpart is demonstrated through numerical results.

***Keywords*-** FDTD algorithm, cold plasma, and Routh-Hurwitz.

I. INTRODUCTON

The finite difference time domain (FDTD) method [1, 2] has prevailed in the computational electromagnetics area as an accurate numerical technique for the direct integration of Maxwell's equations. Its evolution has ensued from several technological developments, resulting in the emergence of various algorithms that extend the method's implementation to various modern applications. A major group of such problems involves pulse propagation inside dispersive materials. Representative examples are the simulation of light propagation in optical devices, soil modeling in ground penetrating radar (GPR) problems [3], and study of potential effects of human tissue exposure to electromagnetic radiation. The techniques that render the FDTD method suitable for dispersive media modeling are grounded on an appropriate formulation of either the equation of motion of charged particles, or the local constitutive relation connecting the dielectric displacement to the electric field. In the former occasion a differential equation, which describes the electric field dependence on the polarization current density, is derived and discretized via regular differencing rules [4, 5]. For the latter case three popular approaches have been presented. The auxiliary differential equation (ADE) [6] technique translates the frequency-dependent constitutive relation in the time domain, by inverse Fourier transform, leading to an ordinary differential equation. The *Z*-transform based method [7] concludes in a similar differential equation, assuming the complex permittivity in the *Z*-domain to be a transfer function. Finally, in the recursive convolution (RC) [1] formulation the convolution integral corresponding to the time domain constitutive relation is approximated by a discrete summation, which is then properly calculated using a recursive procedure. The accuracy of the aforementioned efforts for expanding the FDTD method to frequency dependent materials is controlled by the choice of the spatial increment. Specifically, Yee's scheme is characterized by numerical dispersion errors, which accumulate in time and contaminate the solution. This side-effect is limited by using very fine discretization. Considering the fact that FDTD techniques for dispersive media introduce auxiliary variables or store field values from previous time steps, the fine mesh is translated into excessive memory demands. Furthermore, the achievement of high frequency resolution requires elongated simulations. An obvious way to restrict the memory needs and total computational times is the use of higher-order schemes [8-12]. A fourth-

Submitted On: March 27, 2013
Accepted On: Aug. 16, 2013

order accurate in time and space FDTD approach for propagation in collisionless plasma has been presented in [13-24]. Despite the accuracy and memory savings achieved, the proposed method is restricted to lossless dispersive media. Recently, in [14, 25-31], a novel higher order method for modeling lossy media has been presented. In this paper, a staggered fourth-order accurate in space and second-order accurate in time FDTD scheme for the simulation of lossy dispersive materials is proposed. The media considered are second- and *N*th-order Lorentz, first- and *M*th-order Debye, and second-order Drude. The algorithm is based on the ADE technique [6, 12, 21], while a material-independent perfectly matched layer (PML) [15-18] is utilized for the reflectionless truncation of the computational domain. The stability and numerical dispersion characteristics of the proposed technique, examined for the (2, 2) case in [16, 19, 27, 29, 31], are investigated through the derivation of an appropriate stability criterion as well as a dispersion relation for each material.

II. HIGHER-ORDER FDTD SCHEMES FOR DISPERSIVE MEDIA

The key premise of the proposed FDTD (2, 4) method is the discretization of the spatial and temporal derivatives using fourth-order and second-order approximations, respectively. In order to present a more compact methodology for wave propagation in dispersive media, temporal central finite difference- (δ_t,δ_{2t},δ_t^2), central average- (μ_t,μ_{2t}), and central spatial-operators δ_β are defined in tables I and II. In the context of this paper the spatial derivative $\partial/\partial\beta$ is substituted by the fourth-order spatial operator,

$$\frac{1}{\Delta\beta}\delta_\beta F_m = \frac{1}{24\Delta\beta}$$

$$(F_{m-\frac{3}{2}} - 27F_{m-\frac{1}{2}} + 27F_{m+\frac{1}{2}} - F_{m+\frac{3}{2}}) \quad (1)$$

where the index m corresponds to β coordinate, unless stated otherwise.

The simulation of dispersive materials is founded on the ADE technique. Wave propagation inside the medium is fully described by the two Maxwell's laws, which are discretized using the FDTD (2, 4) scheme, and the frequency-dependent constitutive relation $\boldsymbol{D}(\boldsymbol{r},\omega) = \epsilon(\omega)\boldsymbol{E}(\boldsymbol{r},\omega)$, where $\epsilon(\omega)$ is the complex permittivity defining the material's dispersion properties. Taking the inverse Fourier transform of the previous constitutive relation, an ordinary differential equation is derived, which is then discretized utilizing a central differencing scheme in time. Assuming an *N*th-order dispersion, the process, which has been just described, results in [8-12],

$$E^{n+1} = \mathcal{F}\,(E^n,\ldots,\ E^{n-N+1},\ D^{n+1},\ D^n,\ldots,\ D^{n-N+1}). \quad (2)$$

The two discretized Maxwell's equations along with equation (2) constitute the overall computation model.

Table I: Temporal approximations.

	Time Domain	Z Domain	ωDomain
$\delta_t F^n$	$F^{n+\frac{1}{2}} - F^{n-\frac{1}{2}}$	$Z^{1}/_{2} - Z^{-1}/_{2}$	$2\mathrm{j}\sin(\frac{\omega\Delta t}{2})$
$\delta_{2t} F^n$	$\frac{1}{2}(F^{n+1} - F^{n-1})$	$\frac{1}{2}(\mathrm{Z} - Z^{-1})$	$\mathrm{j}\sin(\omega\Delta t)$
$\mu_t F^n$	$\frac{1}{2}(F^{n+\frac{1}{2}} + F^{n-\frac{1}{2}})$	$\frac{1}{2}(Z^{1}/_{2} + Z^{-1}/_{2})$	$\cos(\frac{\omega\Delta t}{2})$
$\mu_{2t} F^n$	$\frac{1}{2}(F^{n+1} + F^{n-1})$	$\frac{1}{2}(\mathrm{Z} + Z^{-1})$	$\cos(\omega\Delta t)$
$\delta_t^2 F^n$	$F^{n+1} - 2F^n + F^{n-1}$	$\mathrm{Z} + Z^{-1} - 2$	$-4\sin^2(\frac{\omega\Delta t}{2})$

A. Cold plasma media

Cold plasma media is described by the following permittivity function [2, 6, 19, 20],

$$\epsilon(\omega) = \epsilon_0\left[1 + \frac{\omega_p^2}{\omega(j\nu_c - \omega)}\right] \quad (3)$$

where ω_p is the radian plasma frequency and ν_c is the collision frequency. The governing differential equation is,

$$\nu_c\frac{\partial D}{\partial t} + \frac{\partial^2 D}{\partial t^2} = \epsilon_0\,(\omega_p^2 E + \nu_c\frac{\partial E}{\partial t} + \frac{\partial^2 E}{\partial t^2}) \quad (4)$$

which is written in difference notation as,

$$[\, v_c \frac{\delta_{2t}}{\Delta t} + \frac{\delta_t^2}{(\Delta t)^2} \,] D^n =$$

$$\epsilon_0 \,[\, \omega_p^2 \mu_{2t} + v_c \frac{\delta_{2t}}{\Delta t} + \frac{\delta_t^2}{(\Delta t)^2} \,] E^n, \qquad (5)$$

and solved for E^{n+1} to obtain,

$$E^{n+1} = \frac{1}{\epsilon_0}\{\frac{4\epsilon_\infty E^n - \epsilon_0[\omega_p^2(\Delta t)^2 - v_c\Delta t + 2]E^{n-1}}{[\omega_p^2(\Delta t)^2 + v_c\Delta t + 2]} + \frac{1}{\epsilon_0}\{\frac{(2 + v_c\Delta t)D^{n+1} - 4D^n + (2 - v_c\Delta t)D^{n-1}}{[\omega_p^2(\Delta t)^2 + v_c\Delta t + 2]}\}. \qquad (6)$$

Table II: Spatial approximations.

	$\delta_\beta F^m$	Eigenvalues
2nd-order	$F_{m+\frac{1}{2}} - F_{m-\frac{1}{2}}$	$2j \sin(k_{num,\beta} \frac{\Delta\beta}{2})$
4th-order	$-\frac{1}{24}(F_{m+\frac{3}{2}} - F_{m-\frac{3}{2}}) + \frac{9}{8}(F_{m+\frac{1}{2}} - F_{m-\frac{1}{2}})$	$2j[\frac{9}{8}\sin(k_{num,\beta}\frac{\Delta\beta}{2}) - \frac{1}{24}\sin(3k_{num,\beta}\frac{\Delta\beta}{2})]$
6th-order	$\frac{3}{640}(F_{m+\frac{5}{2}} - F_{m-\frac{5}{2}}) - \frac{25}{384}(F_{m+\frac{3}{2}} - F_{m-\frac{3}{2}}) + \frac{75}{64}(F_{m+\frac{1}{2}} - F_{m-\frac{1}{2}})$	$2j[\frac{75}{64}\sin(k_{num,\beta}\frac{\Delta\beta}{2}) - \frac{25}{384}\sin(3k_{num,\beta}\frac{\Delta\beta}{2}) + \frac{3}{640}\sin(5k_{num,\beta}\frac{\Delta\beta}{2})]$

III. STABILITY ANALYSIS

Among the principal properties of the FDTD method, inherent in explicit differential equation solvers, is the conditional stability. In the conventional Yee's scheme the unbounded growth of errors is eluded by the proper choice of the time step size dictated by the Courant condition. The stability characteristics of the proposed higher-order algorithm are investigated using the methodology presented in [17-21, 28-36], which combines the Von Neumann method with the Routh-Hurwitz criterion. It is presumed that the error present in the computation of any field quantity F is described by a single term of a Fourier series expansion,

$$F^n = F_0 Z^n e^{j\sum_{\beta=x,y,z} k_{num,\beta} m\Delta\beta} \qquad (7)$$

where the complex variable Z corresponds to the growth factor of the error. Under this assumption, the temporal differencing and averaging operators as well as the spatial differencing operators are evaluated as shown in tables I and II. The time-dependent wave equation in a source-free homogeneous dispersive medium is,

$$\mu \frac{\partial^2 D}{\partial t^2} - \nabla^2 E = 0 \qquad (8)$$

and approximated by,

$$\mu \frac{\delta_t^2}{(\Delta t)^2} D^n - \sum_{\beta=x,y,z} \frac{\delta_\beta^2}{(\Delta\beta)^2} E^n = 0 \qquad (9)$$

where δ_β, ($\beta = x, y, z$) denotes the central spatial difference operator of arbitrary order with respect to the coordinate indicated by the subscript. Solutions of the form in equation (7) are substituted in equation (9) leading to a polynomial in Z. The stability of the finite difference scheme is assured if the roots of this characteristic polynomial are located inside or on the unit circle in the Z-plane, namely $|Z| \leq 1$. The bilinear transformation,

$$Z = \frac{r+1}{r-1} \qquad (10)$$

is then applied to the stability polynomial. In this way, the exterior of the unit circle in the Z-plane is mapped on the right-half of the r-plane. In order to examine whether the root of the polynomial with respect to r are nonnegative, the Routh table is created. If the values of all the elements in the first column are positive or zero, the algorithm is stable. The enforcement of the stability constraint regarding the specified entries of the Routh table results in certain inequalities relating the parameters of the FDTD scheme. Following the procedure, which has just been described, equation (9) is formulated, with the use of tables I and II as,

$$(Z-1)^2 D_0 + 4Z\epsilon_\infty v^2 E_0 = 0 \qquad (11)$$

where,

$$v^2 = (c_\infty \Delta t)^2 \sum_{\beta=x,y,z} \frac{1}{(\Delta\beta)^2}[\frac{9}{8}\sin(k_{num,\beta}\frac{\Delta\beta}{2}) - \frac{1}{24}\sin(k_{num,\beta}\frac{3\Delta\beta}{2})]^2 \qquad (12)$$

for fourth-order accuracy in space and $c_\infty = 1/\sqrt{\mu\epsilon_\infty}$. A formula similar to equation (12) can be derived in a straight forward manner for any spatial approximation order [29-34]. The spatial discretization operators are shown in table II for the case of second- and sixth-order. Next, the stability properties of the FDTD (2, 4) scheme for

the three aforementioned cold plasmas media will be examined. In the case of the Drude model the methodology will be presented in detail, while for the Debye and Lorentz models only the final results will be provided. The constitutive relation in the *Z*-domain for the Drude model is,

$$\{ [\frac{v_c}{2\Delta t} + \frac{1}{(\Delta t)^2}] Z^2 - \frac{2}{(\Delta t)^2} Z + \frac{1}{(\Delta t)^2} - \frac{v_c}{2\Delta t} \} D_0 = \epsilon_0 \{ [\frac{\omega_p^2}{2} + \frac{v_c}{\Delta t} + \frac{1}{(\Delta t)^2}] Z^2 - \frac{2}{(\Delta t)^2} Z + \frac{\omega_p^2}{2} - \frac{v_c}{\Delta t} + \frac{1}{(\Delta t)^2} \} E_0 \quad (13)$$

Solving equation (11) for D_0 results in,

$$D_0 = -\frac{4Z\epsilon_0 v^2}{(Z-1)^2} E_0 . \quad (14)$$

Substituting in equation (13) the characteristic stability polynomial is derived,

$$S(Z) = [\frac{2}{(\Delta t)^2} + \frac{v_c}{\Delta t} + \omega_p^2] Z^4 + [\frac{8(1-v^2)}{(\Delta t)^2} - \frac{2v_c(1-2v^2)}{\Delta t} - 2\omega_p^2] Z^3 + [\frac{12}{(\Delta t)^2} + 2\omega_p^2 - \frac{16v^2}{(\Delta t)^2}] Z^2 + [\frac{8(1-v^2)}{(\Delta t)^2} - \frac{2v_c(1-2v^2)}{\Delta t} - 2\omega_p^2] Z + \frac{2}{(\Delta t)^2} - \frac{v_c}{\Delta t} + \omega_p^2 . \quad (15)$$

After applying the billinear transformation, we obtain,

$$S(r) = \frac{2v^2 v_c}{\Delta t} r^3 + [\omega_p^2 + \frac{4v^2}{(\Delta t)^2}] r^2 + \frac{2v_c}{\Delta t} (1- v^2) + \omega_p^2 + \frac{4}{(\Delta t)^2} - \frac{4v^2}{(\Delta t)^2} \quad (16)$$

and the corresponding Routh table is built.

Table III: Routh-Hurwithz table.

$\frac{2v^2 v_c}{\Delta t}$	$\frac{2v_c}{\Delta t}(1- v^2)$
$\omega_p^2 + \frac{4v^2}{(\Delta t)^2}$	$\omega_p^2 + \frac{4}{(\Delta t)^2} - \frac{4v^2}{(\Delta t)^2}$
c_3	0
c_5	0

where,

$$c_3 = \frac{2\omega_p^2 v_c}{\Delta t} \frac{1-2v^2}{\omega_p^2 + \frac{4v^2}{(\Delta t)^2}}, \; c_5 = \omega_p^2 + \frac{4(1-v^2)}{(\Delta t)^2} . \quad (17)$$

Enforcing the entries of the first column to be nonnegative we get,

$$v^2 \le 1/2 . \quad (18)$$

In order to derive the numerical dispersion relation, the following discrete solution is assumed,

$$F^n (I, J, K) = F_0 \exp [j (n\omega\Delta t + Ik_{num,x}\Delta x + Jk_{num,y}\Delta y + Kk_{num,z}\Delta z)] \quad (19)$$

where $\boldsymbol{F}$ represents the electric or magnetic field, indexes *I, J, K* denote the position of the nodes in the mesh, $\Delta\beta$ (β=*x, y, z*) are the sizes of the discretization cell, and $k_{num,\beta}$ (β = *x, y, z*) the wave numbers of the discrete modes in the β-direction. Similarly to the continuous case, we replace in Maxwell's equations $\partial/\partial t$ with $j\omega_{num}$ and $\nabla$with $-j\boldsymbol{k}_{num}$, where $\omega_{num} = \frac{2}{\Delta t}\sin(\frac{\omega\Delta t}{2})$. Given ω_{num} and $\boldsymbol{k}_{num}$, Maxwell's equations can be written in discrete form as,

$$\omega_{num}\mu_0 H_0 = \boldsymbol{k}_{num} \times E_0 \quad (20\text{-a})$$

$$\omega_{num}\epsilon_{num}(\omega_{num})E_0 = -\boldsymbol{k}_{num} \times H_0, \quad (20\text{-b})$$

where ϵ_{num} is the discrete permittivity function defined below. The numerical wave number $\boldsymbol{k}_{num}$ derived for the second-order spatial approximation is,

$$\boldsymbol{k}_{num} = \sum_{\beta=x,y,z} \frac{2}{\Delta\beta} \sin(\frac{k_{num,\beta}\Delta\beta}{2}) \alpha_\beta \quad (21)$$

and for the fourth-order spatial approximation,

$$\boldsymbol{k}_{num} = \sum_{\beta=x,y,z} \frac{2}{\Delta\beta} [\frac{9}{8}(\frac{k_{num,\beta}\Delta\beta}{2}) - \frac{1}{24}\sin(\frac{3k_{num,\beta}\Delta\beta}{2})] \alpha_\beta \quad (22)$$

where α_β is the unit vector in β-direction (see table II). The previous definitions can be extended to any order of spatial approximation. The central operator of *N*-order (*N*: even number) has the general form,

$$\delta_\beta F_m = \sum_{j=1(jodd)}^{N-1} c_j^N (F_{m+\frac{j}{2}} - F_{m-\frac{j}{2}}) \quad (23)$$

with the coefficients c_j calculated through Taylor series expansions and given in a closed form [18-24] by,

$$c_j^N = \frac{(-1)^{\frac{j}{2}-\frac{1}{2}}}{2(\frac{j}{2})^2}\frac{[(N-1)!!]^2}{(N-1-j)!!(N-1+j)!!} j = 1, 3, 5, \ldots, N-1 \quad (24)$$

where,

$$n!! = \begin{cases} n.(n-2)\ldots 5.3.1 & n>0, odd \\ n.(n-2)\ldots 6.4.2 & n>0, even \\ 1 & n=-1, 0. \end{cases}$$

Applying the previous formula, the coefficients c_1^2= 1 for Yee's scheme, c_1^4 = 9/8 and c_3^4= −1/24 for Fang's fourth-order scheme, and c_1^6= 75/64, c_3^6= − 25/384, c_5^6= 3/640 for a sixth-order scheme are yielded. It can be easily proven that the numerical wave number for the *N*th-order accurate scheme is,

$$\boldsymbol{k}_{num} = \sum_{\beta=x,y,z}\frac{2}{\Delta\beta}\sum_{j=1(jodd)}^{N-1} c_j^N \sin\left(\frac{j k_{num,\beta}\Delta\beta}{2}\right)\alpha_\beta. \quad (25)$$

The numerical wave number $\boldsymbol{k}_{num}$ is defined as,

$$\boldsymbol{k}_{num} = k_{num}\,(\sin\theta\cos\emptyset\, a_x + \sin\theta\sin\emptyset\, a_y + \cos\theta\, a_z). \quad (26)$$

The discrete counterpart of the continuous permittivity function, called numerical permittivity, is defined as the ratio of the discrete values of *D* and *E*, i.e., $\epsilon_{num} = D^n/E^n$. Similar to the continuous dispersion relation the discrete one is,

$$\mu_0\epsilon_{num}(\omega_{num})\omega_{num}^2 = \boldsymbol{k}_{num}\cdot\boldsymbol{k}_{num} \quad (27)$$

Using the discrete form of the constitutive equation and the temporal operators shown in the third column of table I, which are derived by setting $Z = \exp(j\omega t\Delta t)$, the discrete expression of the complex permittivity function for the cold plasma medium,

$$\epsilon_{num} = \epsilon_0\left[1+\frac{\omega_{p,num}}{\omega_{num}(j\nu_{c,num}-\omega_{num})}\right] \quad (28)$$

where $\omega_{p,num} = \omega_p\sqrt{\cos(\omega\Delta t)}$, $\omega_{num} = \frac{2}{\Delta t}\sin(\frac{\omega\Delta t}{2})$ and $\nu_{c,num} = \nu_c\cos(\frac{\omega\Delta t}{2})$. Restricting ourselves to one-dimensional problems, without loss of generality, it is obtained for the FDTD (2, 2) case,

$$k_{num} = \frac{2}{\Delta}sin^{-1}\left(\frac{\Delta}{2}\omega_{num}\sqrt{\mu_0\epsilon_{num}}\right) \quad (29)$$

for the FDTD (2, 4),

$$\frac{2}{\Delta}\left[\frac{9}{8}\sin\left(\frac{k_{num}\Delta}{2}\right)-\frac{1}{24}\sin\left(\frac{3k_{num}\Delta}{2}\right)\right] = \omega_{num}\sqrt{\mu_0\epsilon_{num}} \quad (30)$$

and for the FDTD (2, 6),

$$\frac{2}{\Delta}\left[\frac{75}{64}\sin\left(\frac{k_{num}\Delta}{2}\right)-\frac{25}{384}\sin\left(\frac{3k_{num}\Delta}{2}\right)+\frac{3}{640}\sin\left(\frac{5k_{num}\Delta}{2}\right)\right] = \omega_{num}\sqrt{\mu_0\epsilon_{num}}. \quad (31)$$

To investigate the dispersive features for both second- and fourth- order schemes we consider the following example in a second order Lorentz medium; let ϵ_∞= 2.25ϵ_0, ϵ_s= 3ϵ_0, ω_0= 2πf_0, f_0= 200 MHz and δ_0= 0.1ω_0. Figure 1 shows the normalized phase velocity $c_{num}/c = k/Re\{k_{num}\}$ for the second-order case with Δ = 0.005 m, *Q* = 0.6 and the fourth- and sixth-order with Δ = 0.01 m, *Q* = 0.1 where the Courant number *Q* is defined as $Q = c_0\Delta t/\Delta$. The superior performance of the higher-order schemes is evident, even for larger Δ.

IV. NUMERICAL RESULTS

The efficiency of the proposed FDTD (2, 4) scheme compared to the conventional second-order accurate technique has been extensively investigated through numerical results. An analytical reference solution has been developed in order to precisely define the potential errors of each method [21-23]. The two schemes have been tested in one-dimensional wave propagation problems in homogeneous and inhomogeneous geometries involving materials of diverse dispersion types. In all the examined cases, the new algorithm has been found to be superior, achieving higher accuracy in modeling dispersive characteristics for equal spatial discretization, or allowing a less dense lattice to be used, while the same level of accuracy is ensured [33-36].

In the first case studied a Lorentz-type medium slab is placed in free space. The resonant frequency of the material is set to $\omega_0 = 2\times 10^9\, rad/sec$, the damping coefficient is equal to δ_0= 0.1ω_0, whereas ϵ_∞= 2.25ϵ_0 and ϵ_s= 3ϵ_0 [22-27]. The wideband reflection coefficient at the interface between air and the dispersive dielectric is calculated by the FDTD (2, 2) and FDTD (2, 4)

ADE techniques. The computational domain consists of 2000 cells and the dielectric slab occupies the region from the 700th cell to 750th cell. For the FDTD (2, 4) scheme the spatial step size is set to Δx = 0.005 m, Q = 0.1 and the total number of time steps N_t = 14250. Two sets of parameters are selected for the FDTD (2, 2) simulations, namely (a) Δx = 0.005 m, Q = 0.95 and N_t= 1500 and (b) Δx = 0.0025 m, Q = 0.95, N_t= 3000 where the number of cells is doubled. The results for the first case are depicted in Fig. 1, along with the reference solution. It is clearly observed that the FDTD (2, 4) scheme is far more accurate obtaining only slight deviations from the exact reflection coefficient function even for frequencies high above the resonant one [25-27]. Contrarily, its (2, 2) counterpart generates significant errors. The reflection coefficient for the latter group of parameters is illustrated in Fig. 2. The graphs corresponding to the two schemes almost coincide introducing minor shifts in the peaks locations compared to the analytical solution. However, it should be reminded that in the FDTD (2, 2) case a two times denser grid is utilized.

In the next simulation, the propagation of the modulated Gaussian pulse $f(t) = \exp\left\{-(t-t_0)^2/T^2\right\}\cos(2\pi f_s t)$ where t_0= 8×10−9 sec, T = 10−9 sec and f_s= 600 MHz, inside a Lorentz-type dispersive medium is explored. The parameters of the material are ω_0= 2π $200\times10^6\, rad/sec$, δ_0= $0.1\omega_0$, ϵ_∞= $2.25\epsilon_0$ and ϵ_s= $3\epsilon_0$. For the FDTD (2, 2) scheme two different uniform grids are considered: (a) Δx = 0.01 m, Q = 0.5 for 5000 time steps and (b) Δx = 0.05 m, Q = 0.5 for 1000 time steps. The respective parameters for the FDTD (2, 4) scheme are Δx = 0.05m and Q = 0.1.

In Fig. 3, the time domain electric field located 0.2 m away from the excitation point is illustrated for the three aforementioned cases along with the exact solution. For an easier observation a detail of the previous graphs is shown in Fig. 4. It is evident that the higher order algorithm achieves the same level of accuracy as the FDTD (2, 2) with the first set of parameter values, but with a five times coarser grid. In table III, the three methods are compared in terms of maximum error and total computational time. It is noted that the proposed higher order technique is more accurate and computationally efficient.

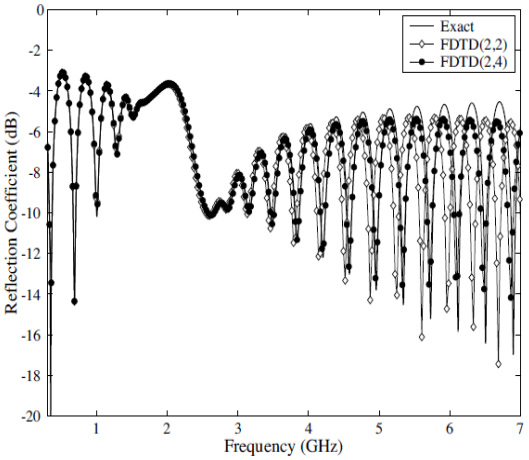

Fig. 1. The reflection coefficient as a function of frequency. Comparison is made between the exact data, FDTD (2, 4) and FDTD (2, 2) with Δx = 0.005 m.

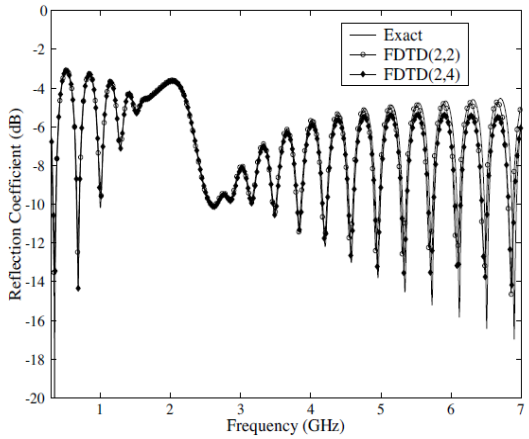

Fig. 2. The reflection coefficient as a function of frequency. Comparison is made between the exact data, FDTD (2, 4) Δx = 0.05 m and FDTD (2, 2) with Δx = 0.0025 m.

Finally, the air-slab problem is solved by the FDTD (2, 2) and FDTD (2, 4) algorithms assuming that the slab is filled with a third order Debye dispersive material. The characteristic parameters of the three poles are ϵ_{s1}= $3\epsilon_0$, τ_1= 9, 4×10^{-9}sec, ϵ_{s2}= $2\epsilon_0$, τ_2= 10^{-10}sec, and ϵ_{s3}=ϵ_0, τ_3 = 10^{-6} sec, while the infinite permittivity is set equal to 2.25 ϵ_0. In both cases, the computational space consists of 2000 cells, the spatial step size is 0.01m and Q = 0.8. The electric

field function in the time-domain is presented in Fig. 5. It is again obvious that the proposed higher order scheme accomplishes better accuracy.

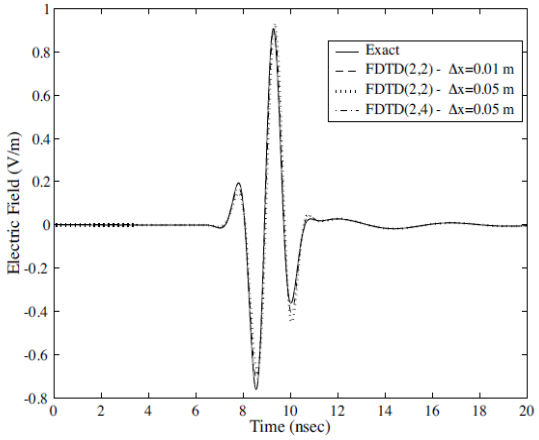

Fig. 3. Electric field waveforms of the exact, FDTD (2, 4) and FDTD (2, 2) with two different grids.

Having verified that FDTD (2, 4) can be efficiently extended to cold plasma medias, it is applied to wave scattering by an infinite height cylinder made of cold plasma placed in air. The computational space consists of 200×200 cells. The cylinder is excited by a plane wave. The wave front is assumed to be a modulated Gaussian pulse centered at 20 GHz. The excitation frequency is stable, while for the plasma frequency of the cold plasma three values have been selected, namely 28.7 GHz, 5.74 GHz, and 0.287 GHz.

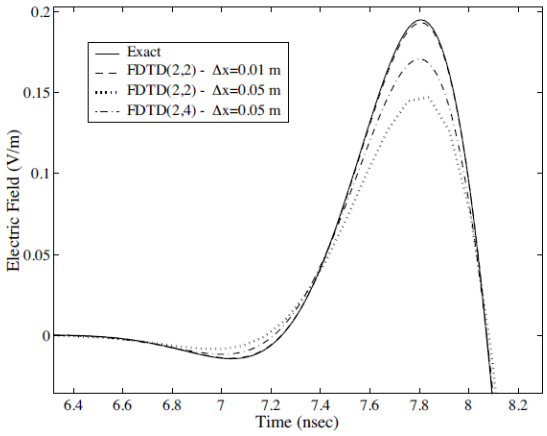

Fig. 4. Details of Fig. 3, observed that the proposed technique produces an acceptable close to the (2, 2) scheme result but with a five-times coarser grid.

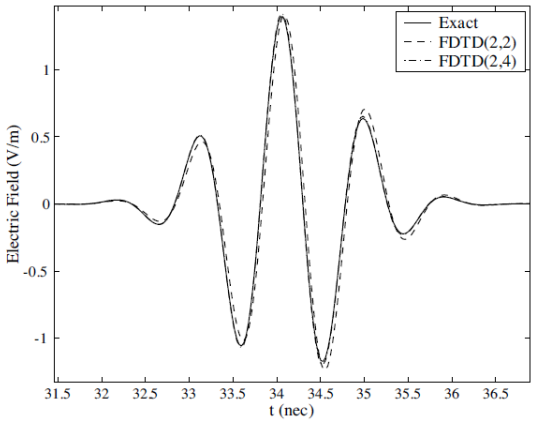

Fig. 5. Electric field waveforms of the exact, FDTD (2, 4) and FDTD (2, 2).

V. CONCLUSION

A novel FDTD (2, 4) scheme for the simulation of wave propagation inside cold plasma media has been presented. Its stability properties for three specific models have been investigated and appropriate stability conditions have been derived. Additionally, the numerical dispersion characteristics have been examined and for the case of a second-order Lorentz medium, it has been verified that the proposed algorithm is more powerful than the conventional second-order technique, as expected. The efficiency of the FDTD (2, 4) algorithm has also been explored in various numerical examples, where it has been compared to the FDTD (2, 2) method and an analytical solution. In all the cases considered, it has been proven that the former achieves better accuracy when the same grid is used or the same level of accuracy for coarser grids. Additionally, the presented method accomplishes minimum errors, while reducing the overall computational time.

REFERENCES

[1] K. Kunz and R. Luebbers, *The Finite Diference Time Domain Method for Electromagnetics*, CRC, Boca Raton, FL, 1993.

[2] A. Taflove and S. Hagness, *Computational Electrodynamics: The Finite-Difference Time-Domain Method*, 2nd ed., Artech House, Boston, MA, 2000.

[3] F. Teixeira, W. Chew, M. Straka, M. Oristaglio, and T. Wang, "Finite-difference time-domain simulation of ground penetrating radar on dispersive, inhomogenous, and conductive soils,"

IEEE Trans. Geosci. Remote Sensing, vol. 36, pp. 1928-1937, Nov. 1998.

[4] J. Young, "Propagation in linear dispersive media: Finite difference time-domain methodologies," *IEEE Trans. Antennas Propagat.*, vol. 43, pp. 422-426, Mar. 1995.

[5] S. Cummer, "An analysis of new and existing FDTD methods for isotropic cold plasma and a method for improving their accuracy," *IEEE Trans. Antennas Propagat.*, vol. 45, pp. 392-400, Mar. 1997.

[6] R. Joseph, S. Hagness, and A. Taflove, "Direct time integration of Maxwell's equations in linear dispersive media with absorption for scattering and propagation of femtosecond electromagnetic pulse," *Opt. Lett.*, vol. 16, pp. 1412-1414, Sept. 1991.

[7] D. Sullivan, "Frequency-dependent FDTD methods using Z transforms," *IEEE Trans. Antennas Propagat.*, vol. 40, pp. 1223-1230, Oct. 1992.

[8] J. Fang, *Time Domain Finite Difference Computation for Maxwell's Equations*, Ph.D. dissertation, University California, Berkeley, CA, 1989.

[9] N. Kantartzis and T. Tsiboukis, "A generalized methodology based on higher-order conventional and non standard FDTD concepts for the systematic development of enhanced dispersionless wide-angle absorbing perfectly matched layers," *International Journal of Numerical Modelling: Electronic Networks, Devices and Fields*, vol. 13, pp. 417-440, 2000.

[10] J. Young, D. Gaitonde, and J. Shang, "Toward the construction of a fourth-order difference scheme for transient EM wave simulation: Staggered grid approach," *IEEE Trans. Antennas Propagat.*, vol. 45, pp. 1573-1580, Nov. 1997.

[11] A. Yefet and P. Petropoulos, "A staggered fourth-order accurate explicit finite difference scheme for the time-domain Maxwell's equations," *J. Comput. Phys.*, vol. 168, pp. 286-315, 2001.

[12] S. Georgakopoulos, C. Birtcher, C. Balanis, and R. Renaut, "Higher-order finite-difference schemes for electromagnetic radiation, scattering, and penetration, Part I: Theory," *IEEE Antennas Propag. Mag.*, vol. 44, pp. 134-142, Feb. 2002.

[13] J. Young, "A higher order FDTD method for EM propagation in a collisionless cold plasma," *IEEE Trans. Antennas Propagat.*, vol. 44, pp. 1283-1289, Sept. 1996.

[14] K. Prokopidis and T. Tsiboukis, "Higher-order FDTD (2, 4) scheme for accurate simulations in lossy dielectrics," *Electron. Lett.*, vol. 39, no. 11, pp. 835-836, 2003.

[15] P. Petropoulos, L. Zhao, and A. Cangellaris, "A reflectionless sponge layer absorbing boundary condition for the solution of Maxwell's equations with high-order staggered finite difference schemes," *J. Comput. Phys.*, vol. 139, pp. 184-208, 1998.

[16] P. Petropoulos, "Stability and phase error analysis of FDTDin dispersive dielectrics," *IEEE Trans. Antennas Propagat.*, vol. 42, pp. 62-69, Jan. 1994.

[17] J. Pereda, L. Vielva, A. Vegas, and A. Prieto, "Analyzing the stability of the FDTD technique by combining the von Neumann method with Routh-Hurwitz criterion," *IEEE Trans. Microwave Theory Tech.*, vol. 49, pp. 377-381, Feb. 2001.

[18] M. Ghrist, *Finite Difference Methods for Wave Equations*, Ph.D. Thesis, University of Colorado at Boulder, Boulder, CO, 2000.

[19] L. Prokopeva, A. Kildishev, J. Fang, J. Borneman, M. Thoreson, V. Shalaev, and V. Drachev, "Nanoplasmonics FDTD simulations using a generalized dispersive material model," *27th Annual Review of Progress in Applied Computational Electromagnetics (ACES)*, pp. 963-968, Williamsburg, Virginia, March 2011.

[20] J. Chen and A. Zhang, "A frequency-dependent hybrid implicit-explicit FDTD scheme for dispersive materials," *Applied Computational Electromagnetics Society (ACES) Journal*, vol. 25, no. 11, pp. 956-961, Nov. 2010.

[21] J. Chen and J. Wang, "A frequency-dependent weakly conditionally stable finite-difference time-domain method for dispersive materials," *Applied Computational Electromagnetics Society (ACES) Journal*, vol. 25, no. 8, pp. 665-671, August 2010.

[22] A. Greenwood, "FDTD model for magnetized plasma," *25th Annual Review of Progress in Applied Computational Electromagnetics (ACES)*, pp. 612-616, Monterey, California, March 2009.

[23] A. Greenwood, A. Schulz, and K. Cartwright, "Hybrid modeling of electromagnetic plasmas," *20th Annual Review of Progress in Applied Computational Electromagnetics (ACES)*, Syracuse, NY, April 2004.

[24] M. pourbagher, J. Nourinia, and N. Pourmahmud, "Reconfigurable plasma antennas," *Indian Journal of Science and T echnology*, vol. 5, no. 6, June 2012.

[25] M. pourbagher, J. Nourinia, and N. Pourmahmud, "Development of a three-dimensional magnetic-field-independent absorbing boundary condition (MFIABC) for cold magneto plasma," *International Journal of Modern Engineering Research*, vol. 2, no. 4, pp. 2880-2884, July 2012.

[26] D. Lawrence and K. Sarabandi, "Electromagnetic scattering from vibrating penetrable objects using a general class of time-varying sheet boundary conditions," *IEEE Trans. Antennas Propagat.*, vol. 54, no. 7, pp. 2054-2061, July 2006.

[27] J.-H. Chang and A. Taflove, "Three-dimensional diffraction by infinite conducting and dielectric wedges using a generalized total-field/scattered-field FDTD formulation," *IEEE Trans. Antennas Propagat.*, vol. 53, no. 4, pp. 1444-1454, April 2005.

[28] S. Tseng, A. Taflove, D. Maitland, and V. Backman, "Pseudospectral time-domain simulations of multiple light scattering in three-dimensional macroscopic random media," *Radio Science*, vol. 41, RS4009, doi:10.1029/2005RS003408, 2006.

[29] J. Simpson and A. Taflove, "Three dimensional FDTD modeling of impulsive ELF propagation about the earth-sphere," *IEEE Trans. Antennas Propagat.*, vol. 52, no. 2, pp. 443-451, Feb. 2004.

[30] J. Simpson, R. Heikes, and A. Taflove, "FDTD modeling of a novel ELF radar for major oil deposits using a three-dimensional geodesic grid of the earth-ionosphere waveguide," *IEEE Trans. Antennas Propagat.,* vol. 54, no. 6, pp. 1734-1741, June 2006.

[31] J. Simpson and A. Taflove, "A review of progress in FDTD Maxwell's equations modeling of impulsive subionospheric propagation below 300 kHz," *IEEE Trans. Antennas Propagat.*, vol. 55, no. 6, pp. 1582-1590, June 2007.

[32] S.-C. Kong, J. Simpson, and V. Backman, "ADE-FDTD scattered-field formulation for dispersive materials," *IEEE Microwave and Wireless Comp. Lett.*, vol. 18, no. 1, pp. 4-6, Jan. 2008.

[33] Y. Yu and J. Simpson, "An E-J collocated 3-D FDTD model of electromagnetic wave propagation in magnetized cold plasma," *IEEE Trans. Antennas Propagat.*, vol. 58, no. 2, pp. 469-478, Feb. 2010.

[34] L. Prokopeva, A. Kildishev, J. Fang, J. Borneman, M. Thoreson, V. Shalaev, and V. Drachev, "Nanoplasmonics FDTD simulations using a generalized dispersive material model," *27th Annual Review of Progress in Applied Computational Electromagnetics (ACES)*, pp. 963-968, Williamsburg, Virginia, March 2011.

[35] J. Chen and A. Zhang, "A frequency-dependent hybrid implicit-explicit FDTD scheme for dispersive materials," *Applied Computational Electromagnetics Society (ACES) Journal*, vol. 25, no. 11, pp. 956-961, November 2010.

[36] J. Chen and J. Wang, "A frequency-dependent weakly conditionally stable finite-difference time-domain method for dispersive materials," *Applied Computational Electromagnetics Society (ACES) Journal*, vol. 25, no. 8, pp. 665-671, August 2010.